Computer Methods and Programs in Biomedicine 204 (2021) 106051

Contents lists available at ScienceDirect

Computer Methods and Programs in Biomedicine

journal homepage: www.elsevier.com/locate/cmpb

Detecting cerebral microbleeds via deep learning with features enhancement by reusing ground truth

Tianfu Li[a,1], Yan Zou[c,1], Pengfei Bai[a,b,*], Shixiao Li[a], Huawei Wang[a], Xingliang Chen[a], Zhanao Meng[c], Zhuang Kang[c], Guofu Zhou[a,b,d]

[a] Guangdong Provincial Key Laboratory of Optical Information Materials and Technology & Institute of Electronic Paper Displays, South China Academy of Advanced Optoelectronics, South China Normal University, Guangzhou 510006, China
[b] National Center for International Research on Green Optoelectronics, South China Normal University, Guangzhou 510006, China
[c] Department of Radiology, The Third Affiliated Hospital of Sun Yat-Sen University, Guangzhou, Guangdong, China
[d] Academy of Shenzhen Guohua Optoelectronics, Shenzhen 518110, China

ARTICLE INFO

Article history:
Received 3 September 2020
Accepted 7 March 2021

Keywords:
Deep learning
Cerebral microbleeds
Feature enhancement
Convolutional neural network
SSD

ABSTRACT

Background and objectives: Cerebral microbleeds (CMBs) are cerebral small vascular diseases and are often used to diagnose symptoms such as stroke and dementia. Manual detection of cerebral microbleeds is a time-consuming and error-prone task, so the application of microbleed detection algorithms based on deep learning is of great significance. This study presents the feature enhancement technology applying to improve the performances of detecting CMBs. The primary purpose of the feature enhancement is emphasizing the meaningful features, leading deep learning network easier and correctly to optimize.

Method: In this study, we applied feature enhancement in detecting CMBs from brain MRI images. Feature enhancement enhanced specific intervals and suppressed the useless intervals of the feature map. This method was applied in SSD-512 and SSD-300 algorithm, using VGG architecture pre-trained in the ImageNet dataset.

Results: The proposed method was applied in SSD-512. Moreover, the model was trained and tested on the sequence of SWAN images of brain MRI images. The results of the experiment demonstrate that our method effectively improves the detection performance of the SSD network in detecting CMBs. We train SSD-512 120000 iterations and test results on the test datasets, by applying the feature enhancement layer, improving the precision with 3.3% and the mAP of 2.3%. In the same way, we trained SSD-300, improving the mAP of 2.0%. 2.8% and 7.4% precision are improved by applying feature enhancement layer In ResNet-34 and MobileNet.

Conclusions: The proposed method achieved more effective performance, demonstrated that feature enhancement can be a helpful algorithm to enhance the deep learning model.

1. Introduction

Cerebral microbleeds (CMBs) are a type of cerebral small vascular disease(CSVD), which is a small and chronic cerebral hemorrhage, the possibility of CMBs increasing with aging [1]. Cerebral microbleeds are often accompanied by stroke [2–4], cerebral amyloid angiopathy [5], neurodegenerative diseases [6], and brain trauma [7]. More importantly, CMBs serve as a sign of potential bleeding tendency for vascular lesions, and the number of CMBs could indicate the risk of future intracranial hemorrhage and hemorrhagic stroke [8], cognitive impairment [9]. Possible pathology may be revealed by the location of CMBs. For example, the large-lobe distribution of CMBs may indicate the possible presence of cerebral amyloid angiopathy [10], while the deep hemisphere or supratentorial CMB may indicate the presence of hypertensive vascular disease [11]. Thus, an accurate and robust model of detecting CMBs is imperatively required.

The performance of detecting CMBs has been enhanced by advances in magnetic resonance imaging (MRI) technology. In paramagnetically sensitive MR sequences such as Susceptibility weighted imaging (SWI) [12,13] or T2 GRE [1]. In the SWI images, paramagnetic blood products are sensitive to be screened. CMBs are observed as a small low-signal hemorrhage point with a diameter

* Corresponding author.
E-mail address: baipf@scnu.edu.cn (P. Bai).
[1] these authors contributed equally to this work

https://doi.org/10.1016/j.cmpb.2021.106051
0169-2607/

between 2-10mm [14]. There are a certain number of mimics that have similar characteristics in SWI, causing by basal neurons vascular cross-section, iron deposition, calcification, signal blanks, etc. [15]. According to statistics, there are more than 100 mimics in an average patient's picture, and markers would spend 5-15 minutes to identify false-positive points and true CMBs [16]. Therefore, manually labeling CMBs is time-consuming and laborious work. It is crucially important to improve the detection performance of the algorithm for detection CMBs which can greatly reduce the workload on radiologists.

To alleviate this problem, many researchers have applied computer vision algorithms in medicine [17]. Ke et al. [18] proposed an adaptive independent subspace analysis (AISA) method using in diagnosis the real autism spectrum disorder. Khan et al. [19] proposed an automated multi-modal method for brain tumor type classification by using deep learning. In recent years developments in deep learning have greatly influenced computer vision and its application in medical image analysis like detection [20–24]. Compared with conventional algorithms, deep learning algorithms generate powerful high-level features through convolution operations to achieve greater performance. In the field of object detection, the common two-step algorithms include Fast R-CNN [25], Mask R-CNN [26], etc., common one-step algorithms include YOLO [27], SSD [28], etc. Compared with the two-step detector, the single-step detector is faster by detecting anchors, eliminating the step for extracting proposals.

In the single-shot framework, SSD has shown its significant performance in object detection, serval different size of feature maps is extracted to be used in detection. Further, a low-level feature map is utilized to detect the small object, while a high-level feature map is utilized to detect the big object. However, the low-level feature map containing the number of basic features and few semantic information results in poor performance of small objects detection, the high-level feature map containing a lack of basic features but meaningful semantic information result in inexactitude location prediction. Furthermore, In SSD, it is not effective to combine the advantages of low-level feature maps and high-level feature maps.

Many researchers had devoted making efforts to detecting CMBs. While utilizing conventional methods to detect CMBs, the conventional image recognition method was a two-step method. The first step was to screen out candidate CMBs, and the second step was to detect CMBs from candidate points. Seghier et al. [29] registered T2 images as a standard template, and then applied a Gaussian mixture model to distinguish CMBs from other brain structures. Barnes et al. [30] extracted candidate points through local statistical thresholding based on intensity, and true CMBs were classified from the candidate points by a trained SVM classifier. Kuijf et al. [16] proposed a method of extracting candidate points by radial symmetry, true CMBs are selected from the candidate points by random forest regression. Using conventional methods to detect CMBs is require an abundant prior knowledge of CMBs. On the other hand, conventional methods capture the low-level features of CMBs, resulting in low accuracy. Therefore, the application of deep learning that can extract advanced features of CMBs to the researches of CMBs has become the focus of researchers, and 3D convolutional neural networks can use spatial information in MRI. Dou et al. [31] trained a CNN model to detect CMBs in SWI, significantly improving the performance of CMBs detections with a sensitivity of 93.2% and precision of 44.3%. Liu et al. [32] used 3D radial symmetry to select candidate points. Then, they used SWI images and phase maps to train the 3D deep convolution model and used quantitative susceptibility mapping and amplitude maps to filter a part of false-positive points. Although the 3D convolution neural network effectively utilizes spatial information, the 3D convolution neural network brings abundant computational burden compared to the 2D convolution neural network.

From using the conventional algorithm to deep convolutional networks algorithm, people have made plenty of contributions in the detection of CMBs. Unlike other objects which have abundant information in natural images, CMBs are observed as a small size of low signal region with little information. In object detection, more superior performance usually achieving by a novel structure of a deeper network. Besides, for extracting higher features, using auxiliary information to enhance CNN has become an effective method. Gidaris and Komodakis et al. [33] using ground-truth in R-CNN to enhance high-level features and enriched the semantic information of the features. He et al. [26] added a semantic segmentation branch trained simultaneously with the object detection backbone in Faster R-CNN. Brazil et al. [34] used high-level features and ground-truth in pedestrian recognition to enrich target features while suppressing background. Derakhshani [35] innovatively proposed the Assisted Excitation of Activations module, which uses ground-truth information to enhance features during the training process of YOLO. As the iterations of training, the degree of enhancement decreases to 0 gradually, which effectively improves the performance of the model. The method above does not require additional information but makes full use of ground-truth to enhance the CNN performance.

The above researches of using auxiliary information to enhance the performance of convolutional neural networks are our motivation to apply feature enhancement in CMBs detection. We propose a method to enhance the features of CMBs and call it to feature enhancement (FE). As shown in Fig. 1, In the process of forwarding propagation, a feature enhancement branch is added to enhance the feature maps, it takes the ground-truth information to enhance the feature maps in a specific area. First, convention image processing is used to convert the ground-truth information to the enhanced masks. This can be considered as an ROI process, according to the pixel intensity of CMBs to select the region that should be activated. Then, the enhanced mask is used to multiply the feature mask with the weight mask which is obtained by the channel normalization of the original feature, and finally, the information in the weight mask is added to the original feature on the channel dimension. This method only changes the training process of the network. In the training process, the information of the true CMBs in the ground-truth is utilized, by using conventional image processing in ground-truth information, helping the network to achieve more effective performance on detecting CMBs. Subsequently, experiments on feature enhancement are performed in the SSD network. The results show that our method effectively improves performance. Furthermore, our method is easy and flexible to be applied to other networks.

2. Materials and methods

For algorithms based on convolutional neural networks, its performance depends on the quality of the dataset. Before introducing the proposed method, we first focused on the data set we used in this study, we converted DICOM files to JPG files. Then CMBs are labeled by several professional researchers. To prevent overfitting, we utilize data augmentation on the data set. To further enhance the performance of the SSD, we apply FE to the VGG-16 backbone. FE first retains the information of CMBs in the ground-truth, excludes information from other areas, and uses conventional image processing methods to retain the important semantic information in a specific interval, and finally enhance the features.

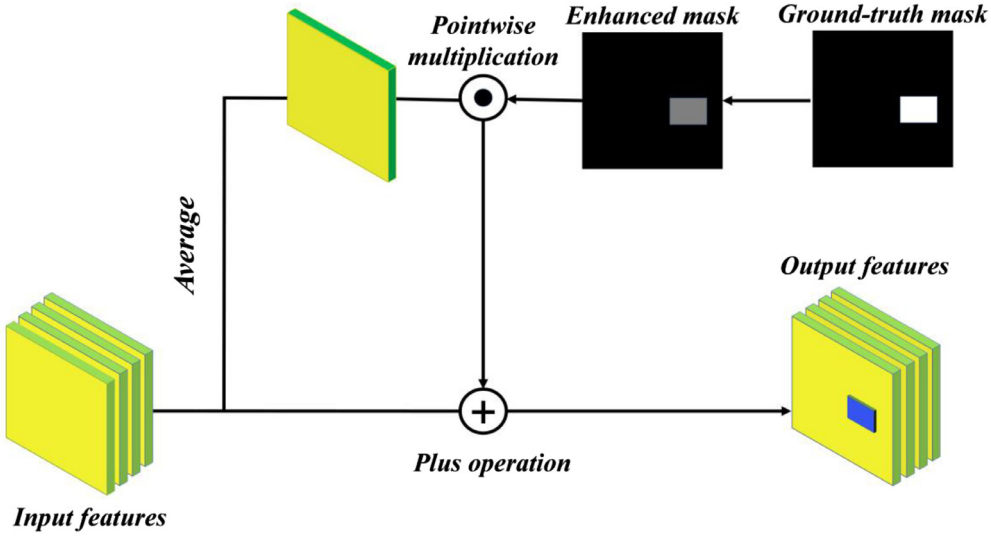

Fig. 1. Feature enhancement process. Using ground-truth bounding box information, each channel of input features is enhanced. Features after processing by enhancing have the same size as input features.

Table 1
Dataset splitting information.

	Patients	Pictures	CMBs
Train	33	467	845
Test	17	167	323
Validation	8	89	133
Total	58	723	1301

2.1. Image acquisition

The data of 58 patients with CMBs were collected by researchers from the third affiliated hospital of sun yat-sen university*, and informed consent was obtained before the scan of each subject. Data were acquired on a 3.0 Tesla scanner (Discovery MR750, GE, Milwaukee, USA), using an 8 channel HRBRAIN coil. The imaging parameters of the T2 FRFSE weighted data were: echo time (TE): 93.0ms; repetition time (TR): 5727ms; echo train length (ETL): 32; bandwidth (BW): 83.3KHz; echo spacing (ES): 1; field of view (FOV): 240mm; number of excitation (NEX): 1.5; matrix size: 512×512; and slice thickness: 5mm. The imaging parameters of the SWAN weighted data were: TE: 45.0ms; TR: 77.3ms; TL: 32; BW: 62.5KHz; flip angle (FA): 15°; FOV: 240mm; NEX: 1; matrix size: 512×512; and slice thickness: 2mm. The imaging parameters of the T2 FLAIR weighted data were: TE: 145.0ms; TR: 8400ms; inversion time (TI): 2100ms; BW: 83.3KHz; FA: 145°; ES: 1; FOV: 240mm; NEX: 1; matrix size: 512×512; and slice thickness: 5mm.

2.2. Data processing

According to statistics, there are 58 patients including 6613 pictures, 723 of which include CMBs. All pictures were labeled by researchers from the Third Affiliated Hospital of Sun Yat-sen University*. These 723 pictures were split into training, validation, and test sets, as shown in Table 1.

To reduce the influence from variation causing by imaging parameters, Advanced Normalization Tools (ANTs) were used to correct the bias effects in magnitude images. After preprocessing SWI images, three experienced neuroradiologists were responsible for labeling each CMB, according to the standard in [1]. Then, Considering the small amount of training data and preventing overfitting, random data augmentation was performed. Data augmentation includes random up-to-down flipping with probability 0.5 and random left-to-right flipping, random magnification of pixel intensity with multiples of [1.2, 1.5], Gaussian blur with a range of [0, 3.0]. in affine transformation, the maximum translation in each direction is 15 pixels, the rotation range is [-30°,30°], and the zoom range is [0.8,0.95]. After the data augmentation, training sets increased to 4434 pictures.

2.3. Method

The feature Enhancement (FE) method we proposed is to enhance the features of the feature map during the training process, thereby helping the network to better learn the features of CMBs. In the testing stage, we still use the original network. For this purpose, we only add our FE layer to the network during training. Relying on the FE layer, the features are continuously enhanced by the ground-truth information, guiding the network to correctly optimize. Since the original network is used for testing, the ground-truth information does not affect the testing stage. The FE layer is shown in Fig. 1.

Focusing on the information of ground-truth, first, ground-truth mask is constructed by the bounding box information of ground-truth as follows:

$$M(i,j) = \begin{cases} P(i,j), if\ object\ in\ this\ pixel \\ 0, if\ no\ object\ in\ this\ pixel \end{cases}$$

P is the image input to the network. This step aims to retain the information of each bounding box and eliminates the information in other areas. for each bounding box in M, the mean value B_{mean} of each area of bounding box B_{area} in M is calculated. Then we use β to control the size of B_{mean} as follow:

$$B_{mean} = \beta * mean(B_{area})$$

Enhanced pixels are determined by B_{mean}. using different β values, the enhancement interval will be different. In this experiment, β is set to 1.5. Pixel values greater than β value will be discarded. Based on the idea that the area with a smaller value will get stronger enhancement, the value of pixels in M is normalized by B_{mean}. Hereafter, the complement number is obtained as follows:

$$M(i,j) = \begin{cases} 1 - \frac{M(i,j)}{B_{mean}}, & if\ the\ object\ in\ this\ pixel \\ 0, & if\ no\ object\ in\ this\ pixel \end{cases}$$

The enhanced mask is obtained by resized of M to the same size of features. given input $X^l_{(c,h,w)}$, we can describe the process

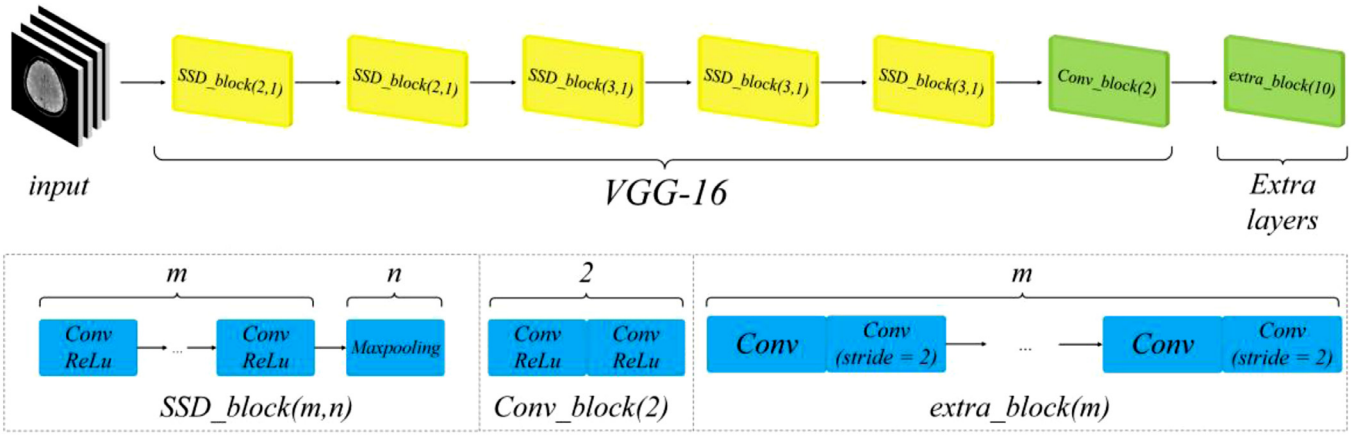

Fig. 2. SSD architecture. The network of SSD includes the VGG-16 backbone and extra layers. Compared with max-pooling of VGG-16 backbone, in extra layers, feature maps are downsampled by convolution with the stride of 2.

of FE as follows, $M(i, j)$ which is rich in information to enhance specific regions, is used to multiply by $X^l_{(c,h,w)}$ and then add to $X^l_{(c,h,w)}$.

$$X^{l+1}_{(c,h,w)} = X^l_{(c,h,w)} + M(i, j) \odot X^l_{(c,h,w)}$$

2.4. Network and settings

We used SSD [28] as our base algorithm, As shown in Fig. 2, SSD was built on the backbone network of VGG-16 and extra layers were added. Based on that, SSD generated a series of feature maps to detect objects. from feature maps from conv4_3 to conv10_2, the object size detected by SSD was from small to big. The lowest layer of the feature maps is the best layer for detecting small objects [36]. Based on assumptions, the following results were obtained by adding the FE layer in conv4_3.

All experiments results were obtained on the deep learning framework of PyTorch v1.1 on the computer equipped with 16GB RAM. NVIDIA RTX2080Ti GPU with 11GB memory was used to accelerate the computation. To focus on the improvement which is brought by FE, the original setting of SSD was kept. Its momentum is 0.1, the learning rate of the first 80k iterations is 1e-3, and it was respectively attenuated by 10 times at 100k and 120k iterations (to 1e-4 and 1e-5). The batch size was set as 4 and the optimizer algorithm "Adam" was used.

3. Experiment results

The process of FE is shown in Fig. 3. (a) shows the picture fed into the SSD-FE network, with the true CMBs information in the yellow rectangular frame. While the iteration increasing to 100k, feature maps of SSD-FE are extracted, then we subtract it from the feature maps input to the FE layer to obtain the specific locations of enhancing by FE layer. (b) shows the area where the FE layer enhances. (c) shows (b) in (a). As shown in Fig. 3, FE enhances the semantic information of the object. In this experiment, each channel of feature maps is enhanced by the FE layer.

In the evaluation of detection CMBs, sensitivity is more important than precision, thus a low threshold is chosen to obtain a useful result with high sensitivity. In this experiment, the same number of pictures that have only mimics were added to test sets. Results of sensitivity-precision are shown in Fig. 4 to compare the performance of SSD and SSD-FE. As is demonstrated in Fig. 4, the performance of SSD-FE is more excellent than SSD. While the sensitivity achieving 90%, the precision of SSD is 76.4%, SSD-FE achieving 79.7%, which improved by 3.3%.

Table 2
AP results of SSD-300 and SSD-512.

Algorithm	Backbone	AP
SSD (300)	VGG-16	0.482
SSD (300)-FE	VGG-16	0.502
SSD (512)	VGG-16	0.733
SSD (512)-FE	VGG-16	0.756

For the reason that the sensitivity- precision curve is easily affected by the number of mimics, therefore Free-response Receiver Operating Characteristic (FROC) curve is used to further compare the performance of SSD and SSD-FE. In the FROC curve, the larger Area Under the ROC Curve (AUC), the better the performance of the model. As shown in Fig. 5, compared with SSD, SSD-FE has a larger AUC, and with the same false-positive rate, there is a higher true positive rate.

Representative false positive points are shown in Fig. 6. False-positive points contain mimics points that are highly similar to true CMBs. These mimics are one of the reasons causing reducing SSD detection precision. But those false positive points are detected by SSD but not by SSD-FE. It means that SSD-FE can better distinguish the part of the mimic's points from CMBs, achieving effective detection performance by reducing the detection of false-positive points.

Table 2 shows FE layer performance in SSD-300 and SSD-512. Compared with SSD-512, SSD-300 obtains lower AP, for the reason that size of input images is smaller than inputs images of SSD-512. On the other hand, the AP of SSD-300 is improved by 2.0%, AP of SSD-512 is improved by 2.3%.

Furthermore, a 10-fold cross-validation method is applied in contrast performance of SSD-FE with SSD. According to the statistics, SSD achieves average precision of 73% and SSD-FE achieves average precision of 75%. Our methods improve the average precision of SSD by 2%.

Table 3 shows that FE outperforms on different backbones in SSD. Precision of VGG-16 is improved 3.3% from 76.4% to 79.7% and 2.8% in ResNet-34. The performance of our MobileNet-based model is significantly improved by the FE, achieving 7.4%.

4. Discussion

Detecting the number and location of CMBs is an important metric for diagnosing CSVD. However, manually labeling CMBs is time-consuming, laborious, and error-prone work. Hence, applying object detection technology in the detection of CMBs can alleviate

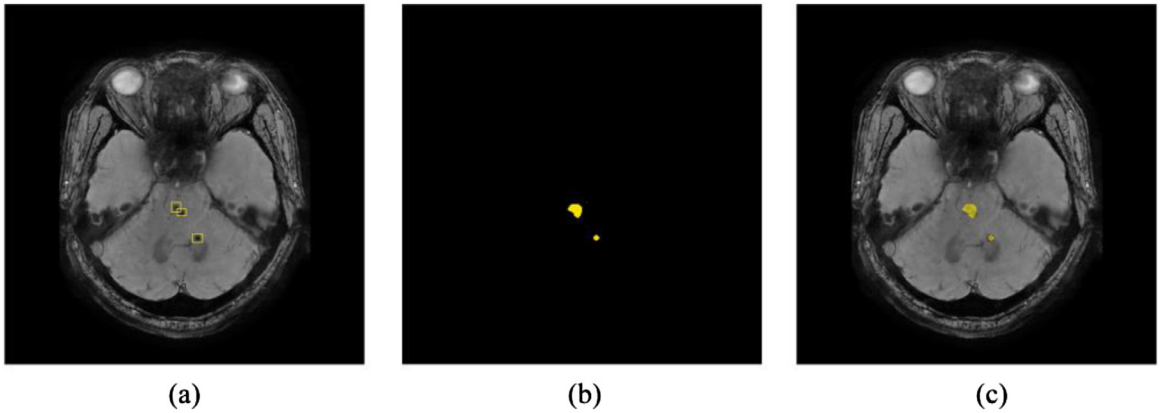

Fig. 3. (a)Image which is fed into the SSD-FE network (with a ground-truth rectangle). (b)Feature enhancement region by ground-truth information. (c) Feature enhancement region in the image.

Table 3
Comparisons of different backbones in SSD with different resolution of input image.

Backbone	Resolution	Recall	Precision	Training Time(second/batch)
VGG-16	512*512*3	90%	76.4%	0.343
VGG-16-FE	512*512*3	90%	79.7%	0.430
MobileNet	320*320*3	90%	42.8%	0.138
MobileNet-FE	320*320*3	90%	50.2%	0.181
ResNet34	300*300*3	90%	70.3%	0.129
ResNet34-FE	300*300*3	90%	73.1%	0.159

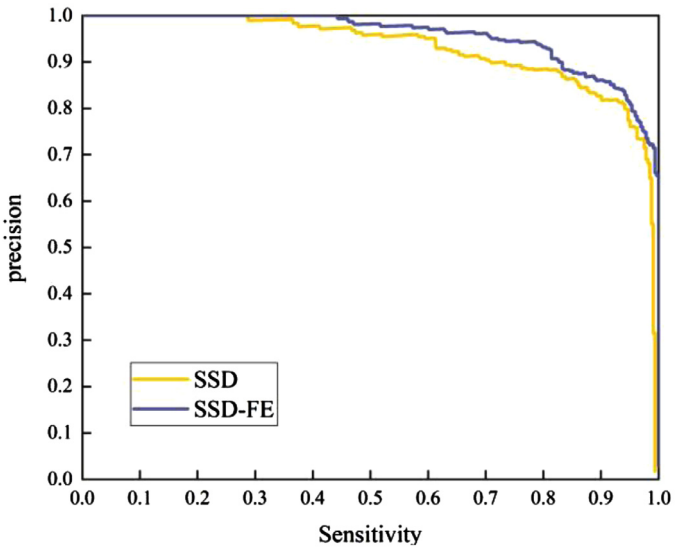

Fig. 4. sensitivity- precision curves of SSD and SSD-FE.

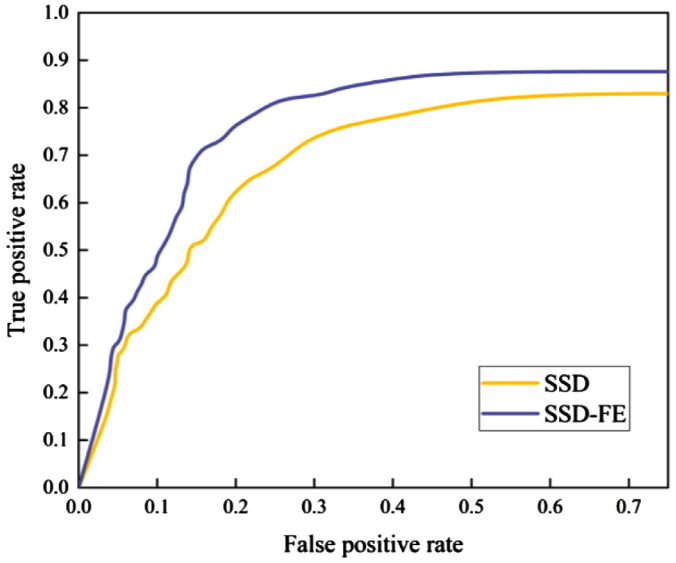

Fig. 5. FROC curves of SSD and SSD-FE.

this problem. A considerable amount of research has been finished during the last few years but still face the challenge in detecting CMBs, including simple feature, small size, and mimics. Detecting CMBs need to be the subject of further study.

In recent years, deep learning yield unusually brilliant results in computer vision, many research studies had been carried out on this topic. More superior than the conventional method, deep learning extracts higher-level features to achieving effective performance. There were many efforts had been probed into extracting features, being devoted to researching deeper networks from AlexNet to DenseNet. Secondly, plenty of processing feature researches had been explored, the object detection algorithm had been developed, including Faster R-CNN, Yolo, SSD. Most object detection algorithms showed superior performance while using natural image datasets. In contrast, algorithms met challenges in using the medical image dataset, including marker staff were required to be equipped with more prior knowledge, and small size of datasets. Training network relies on sufficient datasets, lack of datasets may induce overfitting. On the other hand, a simple feature like CMBs may cause a vanishing gradient problem.

Numerous studies had suggested a novel idea that reusing ground-truth information to enhance the network. Overfitting had been alleviated by data augmentation, reusing ground-truth information kept the features more stable like the effect of the residual block in ResNet [37] and the attention mechanism [38]. In a single-step object detection algorithm, object classification and location regression are performed in feature maps. It relies on location and

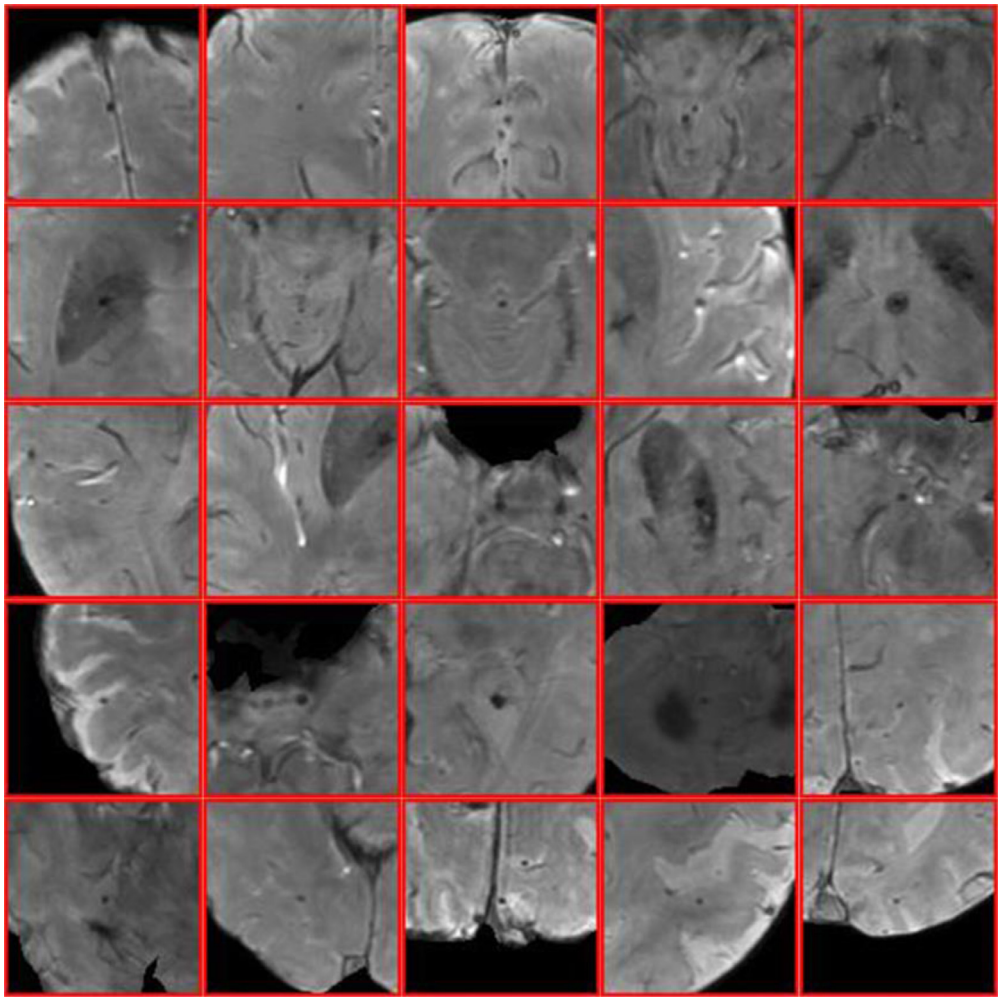

Fig. 6. Representative classification results for CMBs test results, each small picture shows the false positive point which SSD detected, but not by SSD-FE.

semantic information. In this study, the method we proposed can improve both location and semantic information of CMBs, guiding SSD easier to study the features of CMBs. Unlike other global enhancement strategies, FE enhances the specific region by consulting ground-truth information. Weaker the feature, the stronger the enhancement. As a result, the feature of CMBs would be better enhanced, the other region would be less enhanced.

Previous experiments in this study have proven that SSD with the FE layer shows more effective performance in detecting CMBs. To further justify the effectiveness of the FE layer, average precision (AP) is using as the quantified metric for models. Results demonstrate that FE layers can also be applied in a different algorithm like SSD-300 which have different size of input images. Besides, the result shows that SSD-512 achieves more effective performance than SSD-300. Disparity performance could be attributed to the size of input images.

In deep neural networks, as the network deepens, the high-level feature layers have Abundant semantic information. In feature space, the distance between the distribution of the true positives and false positives is determined by the performance of the model [39]. Hence, high-level feature layers are considered suitable layers for the classification task. However, due to the need for down sampling [40], feature maps are transformed into smaller and smaller. In high-level feature maps, the small object is located in a very small area. Therefore, high-level feature maps are not the optimal feature map for the detection of small objects, which is one of the reasons why objects detection algorithms perform not excellent in detecting the small object. As shown in Fig. 7, SSD-FE shows its effectiveness in detecting small CMB that could not be detected by SSD, which is one of the reasons why FE improves the performance of SSD.

Table 4
comparison of different studies.

Algorithm	Sensitivity	precision	FP/CMB
SSD (512)	90%	76.4%	0.31
SSD (512)-FE	90%	79.7%	**0.23**
Liu et al. [32]	95.8%	70.9%	0.39
Chen et al. [41]	94.7%	71.9%	11.7

We run SSD with the different backbone to quantitively evaluate the training speed. In our machine, with an Nvidia RTX 2080Ti GPU to accelerate the training speed. FE only changes the training process of the network, so we counted the time consumed by once forward propagation, As shown in Table 3, FE brings an extra 26% calculation time but outperforms effectively. Note that we keep the same Batchsize 8 in each experiment group.

As shown in Table 4, our SSD-FE model achieving similar performance with He et al. However, Due to the different datasets, FP/CMB can more accurately indicate the performance of the model, and a smaller FP/CMB indicates better model performance. In this study, our model reached 0.24FP/CMB, indicating that our model is better than Liu et al's 0.39 and Chen et al's 11.6.

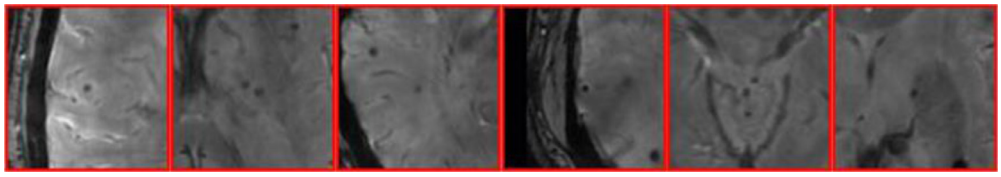

Fig. 7. Representative results of Small CMBs detected by SSD-FE but not by SSD.

Although this study completes the application of FE in SSD and improved the detection performance of SSD for CMBs, this study still has some limitations. In this study, only SWI sequences were used to detect CMBs, but the false-positive samples brought by the calcification can be distinguished by SWI filtered phase images [42]. In the future, we take into comprehensively consideration using multiple sequence information, to exclude the influence of some false positive samples. Second, the confidence of detecting small objects is lower than big objects. Performance in detecting small objects could be furtherly improved by scale-variant templates [36] and other methods. Third, there is a lack of public data sets similar to PASCAL VOC or MS COCO in this field, and the performance of the model in deep learning relies heavily on the quality of the dataset, so the comparison of the conclusions obtained by different studies lacks credibility. Fourth, although FE is proven effective in SSD with different backbone networks such as VGG, MobileNet and ResNet, it lacks experimental results on other algorithms such as Faster RCNN or YOLO. On the other hand, it has been proven to be effective to use FE in improving the performance of SSD. However, to apply the results to the clinic, it is necessary to explore more reasonable parameter settings and more feature enhancement methods.

5. Conclusion

In this paper, we proposed a novel method to enhance SSD performance in detecting Cerebral microbleeds by feature enhancement. The feature enhancement layer emphasizes the value of feature maps. in other words, low-level feature maps are enhanced by semantic information. By using abundant location and semantic information, SSD shows its effective performance. Quantitative evaluation results demonstrate Superior performance by using feature enhancement. in this study, we experimented to demonstrate the performance improvement of SSD-FE on our own CMBs dataset. Besides, FE can bring performance improvements on different backbones, while only adding some computing time. On the other hand, this method is flexible, easily integrated into different CNN architectures. According to finetuning the parameters, not only a single-stage or two-stage algorithm but also other algorithm based on CNN in the field of computer vision can be improved by feature enhancement.

Declaration of Competing Interest

The authors declared that they have no conflicts of interest to this work.

Acknowledgments

This work was supported by Zhongshan Innovative Research Team Program (180809162197886), Program for Chang Jiang Scholars and Innovative Research Teams in Universities (No. IRT_17R40), Program for Guangdong Innovative and Enterpreneurial Teams (No. 2019BT02C241), Science and Technology Program of Guangzhou (No. 2019050001), Guangdong Provincial Key Laboratory of Optical Information Materials and Technology (Grant No. 2017B030301007), MOE International Laboratory for Optical Information Technologies, Guangzhou Key Laboratory of Electronic Paper Displays Materials and Devices and the 111 Project.

References

[1] JM Wardlaw, EE Smith, GJ Biessels, C Cordonnier, F Fazekas, R Frayne, et al., Neuroimaging standards for research into small vessel disease and its contribution to ageing and neurodegeneration, Lancet Neurol. 12 (2013) 822–838, doi:10.1016/S1474-4422(13)70124-8.
[2] Z Chen, Y Ding, X Ji, X Yin, R Meng, Advance of antithrombotic treatment in patients with cerebral microbleed, J. Thromb. Thrombol. (2020).
[3] SA Mayer, NC Brun, J Broderick, SM Davis, MN Diringer, BE Skolnick, et al., Intracerebral, Hemorrhage. Stroke 34 (2018) 224–229.
[4] Microbleeds, Cerebral hemorrhage, and functional outcome after stroke thrombolysis, Stroke (2017).
[5] RJ Cannistraro, JF. Meschia, The clinical dilemma of anticoagulation use in patients with, Cereb. Amyloid Angiopathy Atrial Fibrillation 40 (2018) 1–9.
[6] TA Polyakova, OS. Levin, Cerebral microbleeds in cerebrovascular and neurodegenerative diseases with cognitive impairments, Neurosci. Behav. Physiol. 47 (2017) 1–8.
[7] Andrei I, Ammar D, Van N, David R, Kenneth R. Age, sex and cerebral microbleed effects on white matter degradation after traumatic brain injury. Innov. Aging n.d.:Supplement_1.
[8] HF Yu, Z Lei, WWM Lam, VCT Mok, KS. Wong, Cerebral microbleeds as a risk factor for subsequent intracerebral hemorrhages among patients with acute ischemic stroke, Stroke 34 (2003) 2459–2462.
[9] MMF Poels, MA Ikram, H.A Van A. der L, WJ Niessen, GP Krestin, et al., Cerebral microbleeds are associated with worse cognitive function: the rotterdam scan study, Neurology 78 (2012) 326–333.
[10] A Charidimou, D. Werring, Cerebral microbleeds: Detection, mechanisms and clinical challenges, Fut. Neurol. 6 (2011) 587–611, doi:10.2217/fnl.11.42.
[11] PB Gorelick, A Scuteri, SE Black, C Decarli, SM Greenberg, C Iadecola, et al., AHA /ASA scientific statement vascular contributions to cognitive impairment and dementia a statement for healthcare professionals from the, Am. Heart Asso. / Am. Stroke Asso. (2011) 2672–2713, doi:10.1161/STR.0b013e3182299496.
[12] JR Reichenbach, R Venkatesan, DJ Schillinger, DK Kido, EM. Haacke, Small vessels in the human brain: MR venography with deoxyhemoglobin as an intrinsic contrast agent, Radiology 204 (1997) 272–277.
[13] EM. Haacke, Susceptibility weighted imaging (SWI), Magn. Reson. Med. 16 (2006) 237.
[14] SM Greenberg, MW Vernooij, C Cordonnier, A Viswanathan, R Al-Shahi Salman, S Warach, et al., Cerebral microbleeds: a guide to detection and interpretation, Lancet Neurol. 8 (2009) 165–174, doi:10.1016/S1474-4422(09)70013-4.
[15] C Charlotte, ASS Rustam, W Joanna, Spontaneous brain microbleeds: systematic review, subgroup analyses and standards for study design and reporting, Brain. A J. Neurol. (2007) 8.
[16] HJ Kuijf, J de Bresser, MI Geerlings, MMA Conijn, MA Viergever, GJ Biessels, et al., Efficient detection of cerebral microbleeds on 7.0t mr images using the radial symmetry transform, Neuroimage 59 (2012) 2266–2273, doi:10.1016/j.neuroimage.2011.09.061.
[17] T Liu, W Fan, C. Wu, A hybrid machine learning approach to cerebral stroke prediction based on imbalanced medical dataset, Artif. Intell. Med. 101 (2019).
[18] Woźniak M. Adaptive independent subspace analysis of brain magnetic resonance imaging data 2019 7. https://doi.org/10.1109/ACCESS.2019.2893496.
[19] Khan MA, Ashraf I, Damasevicius R, Scherer R. Multimodal brain tumor classification using deep learning and robust multimodal brain tumor classification using deep learning and robust feature selection : a machine learning application for radiologists 2020. https://doi.org/10.3390/diagnostics10080565.
[20] Wolterink JM, Leiner T, De Vos BD, Van Hamersvelt RW, Viergever MA, I?Gum IBT-IC on MIC & CI. Automatic coronary artery calcium scoring in cardiac CT angiography using paired convolutional neural networks, 2016.
[21] Kuan K, Ravaut M, Manek G, Chen H, Lin J, Nazir B, et al. Deep learning for lung cancer detection: tackling the kaggle data science bowl 2017 challenge 2017.
[22] Nppi JJ, Hironaka T, Regge D, Yoshida HBT-SMI. Deep transfer learning of virtual endoluminal views for the detection of polyps in CT colonography, 2016.
[23] R Holger, Le Roth, J. Lu, et al., Improving computer-aided detection using convolutional neural networks and random view aggregation, IEEE Trans. Med. Image. (2016).
[24] T Kooi, G Litjens, B Van Ginneken, A Gubern-Mérida, CI Sánchez, R Mann, et al., Large scale deep learning for computer aided detection of mammographic lesions, Med. Image Anal. 35 (2017) 303–312.

[25] S Ren, K He, R Girshick, J. Sun, Faster R-CNN: towards real-time object detection with region proposal networks, IEEE Trans. Pattern Anal. Mach. Intell. 39 (2017) 1137–1149, doi:10.1109/TPAMI.2016.2577031.
[26] K He, G Gkioxari, P Dollár, R. Girshick, R-CNN. Mask, IEEE Trans. Pattern Anal. Mach. Intell. 42 (2020) 386–397, doi:10.1109/TPAMI.2018.2844175.
[27] Redmon J, Farhadi A. YOLOv3: an incremental improvement 2018.
[28] W Liu, D Anguelov, D Erhan, C Szegedy, S Reed, CY Fu, et al., in: SSD: Single Shot Multibox Detector. Lect Notes Comput Sci (Including Subser Lect Notes Artif Intell Lect Notes Bioinformatics), LNCS, 2016, pp. 21–37, doi:10.1007/978-3-319-46448-0_2. 9905.
[29] ML Seghier, MA Kolanko, AP Leff, HR Jäger, SM Gregoire, DJ. Werring, Microbleed detection using automated segmentation (MIDAS): a new method applicable to standard clinical MR images, PLoS One 6 (2011) 1–9, doi:10.1371/journal.pone.0017547.
[30] SRS Barnes, EM Haacke, M Ayaz, AS Boikov, W Kirsch, D. Kido, Semiautomated detection of cerebral microbleeds in magnetic resonance images, Magn. Reason. Image. 29 (2011) 844–852, doi:10.1016/j.mri.2011.02.028.
[31] Q Dou, H Chen, L Yu, L Zhao, J Qin, D Wang, et al., Automatic detection of cerebral microbleeds from MR images via 3D convolutional neural networks, IEEE Trans. Med. Image. 35 (2016) 1182–1195, doi:10.1109/TMI.2016.2528129.
[32] S Liu, D Utriainen, C Chai, Y Chen, L Wang, SK Sethi, et al., Cerebral microbleed detection using susceptibility weighted imaging and deep learning, Neuroimage (2019), doi:10.1016/j.neuroimage.2019.05.046.
[33] S Gidaris, N. Komodakis, Object detection via a multi-region and semantic segmentation-aware U model, Proc. IEEE Int. Conf. Comput. Vis. (2015) 1134–1142 2015 Inter:, doi:10.1109/ICCV.2015.135.
[34] G Brazil, X Yin, X. Liu, Illuminating pedestrians via simultaneous detection and segmentation, Proc IEEE Int Conf Comput Vis (2017) 4960–4969 2017-Octob, doi:10.1109/ICCV.2017.530.
[35] Derakhshani MM, Masoudnia S, Shaker AH, Mersa O. Assisted excitation of activations : a learning technique to improve object detectors n.d.:9201–10.
[36] Hu P, Ramanan D. Finding tiny faces. Proc - 30th IEEE Conf Comput Vis Pattern Recognition, CVPR 2017 2017; 2017 -Janua:1522–30. https://doi.org/10.1109/CVPR.2017.166.
[37] He K, Zhang X, Ren S, Sun J. Deep residual learning for image recognition 2015.
[38] J Hu, L Shen, S Albanie, G Sun, E. Wu, Squeeze-and-excitation networks, IEEE Trans. Pattern Anal. Mach. Intell. 42 (2020) 2011–2023, doi:10.1109/TPAMI.2019.2913372.
[39] C Cortes, VN. Vapnik, Support vector networks, Mach Learn 20 (1995) 273–297.
[40] Boureau YL, Ponce J, Lecun YBT-IC on ML. A Theoretical analysis of feature pooling in visual recognition, 2010.
[41] Y Chen, JE Villanueva-Meyer, MA Morrison, JM. Lupo, Toward automatic detection of radiation-induced cerebral microbleeds using a 3D deep residual network, J. Digit. Image. (2019) n.d..
[42] W Zhen, S Mittal, K Kish, Y Yu, J Hu, EM. Haacke, Identification of calcification with MRI using susceptibility-weighted imaging: a case study, J. Magn. Reason Image. Jmri 29 (2009) 177–182.